Literatur

[1] A. G. Gaydon und H. G. Wolfhard, Flames – Their Structure, Radiation and Temperature, 2nd ed., Chapman & Hall, London 1960.
[2] J. H. Bechtel, Appl. Opt. *18*, 2100 (1979).
[3] R. W. Dibble und R. E. Hollenbach, 18th Symposium (International) on Combustion, p. 1489, The Combustion Institute, Canada 1981.
[4] J. R. Smith, SAE paper 820043.
[5] A. C. Eckbreth, 18th Symposium (International) on Combustion, p. 1471, The Combustion Institute, Canada 1981.
[6] J. H. Bechtel und A. R. Chraplyvy, Proc. IEEE *70*, 658 (1982).
[7] D. A. Greenhalgh, International Conference on Combustion in Engineering, The Institute of Mech. Eng., Oxford 1983.
[8] D. V. Murphy, M. B. Long, R. K. Chang und A. C. Eckbreth, Opt. Lett. *4*, 167 (1979).
[9] B. Saggau, 19th Symposium (International) on Combustion, p. 503, The Combustion Institute, Israel 1982.
[10] D. R. Crosley, J. Chem. Educ. *59*, 446 (1982).
[11] R. W. Schmieder und A. Kerstein, Appl. Opt. *19*, 4210 (1980).
[12] R. W. Schmieder, Sandia-Report SAND 81-8886 (1982).
[13] D. R. Crosley, Opt. Eng. *20*, 511 (1981).
[14] H. Herzberg, Molecular Spectra and Molecular Structure, Van Nostrand Reinhold Company, New York 1950.
[15] F. Wesner, ETZ-A *91*, 511 (1970).
[16] G. Tsatsaronis, Combust. Flame *33*, 217 (1978).
[17] G. E. Andrews und D. Bradley, Combust. Flame *19*, 275 (1972).
[18] G. Dixion-Lewis und M. J. W. Wilson, Trans. Faraday Soc. *46*, 1106 (1951).
[19] G. Janisch, Chem.-Ing.-Tech. *43*, 561 (1971).

E 5507

Laser-Induced Saturated Fluorescence as a Method for the Determination of Radical Concentrations in Flames

K. Kohse-Höinghaus, W. Perc, and Th. Just

Institut für Physikalische Chemie der Verbrennung. DFVLR, Pfaffenwaldring 38, 7000 Stuttgart 80, West Germany

Flammen / Fluoreszenz / Freie Radikale

The laser-induced saturated fluorescence method was further developed with the aim of increasing the accuracy of radical concentration measurements in flames. Absolute number densities for CH and OH in a low-pressure acetylene/oxygen flame were obtained from saturation curves based on a two-level rate equation model, whose validity was checked for the experimental conditions. From these saturation curves, approximate oscillator strengths could be deduced, which could serve as a cross-check for the evaluated number densities. Temperatures were determined from rotational spectra of the excited molecules. – For CH as well as for OH, the concentrations obtained with different excitation methods agree well with each other. They were compared with kinetic model calculations. For the extension of the saturated fluorescence method to higher pressures, a multi-level model is being developed.

Introduction

Saturated fluorescence using high power densities of the exciting laser has several advantages over the linear fluorescence method: for complete saturation the detectable signal is maximized, and the peak fluorescence intensity is insensitive to collisional quenching and relaxation as well as to laser intensity fluctuations.

Since this method was proposed by Piepmeier [1] and Daily [2], several quantitative saturated fluorescence experiments on flame radicals as C_2 [3, 4], CH [4–6], CN [5, 6], OH [7], and NH [8] have been described. Mostly, atmospheric pressure flames have been investigated [3, 5, 6]. For some of those experiments, the results have been compared with absorption measurements, giving typical discrepancies of factors of two to five [5, 6]. These large errors are partly due to oversimplified assumptions. As for molecules in most cases only a partial saturation can be achieved, collision processes are not negligible. For atmospheric pressure flames, the representation by a two-level model, which does not include rotational energy transfer, can lead to considerable misinterpretations of the experimental data. Most recently, Morley [9] comes to the conclusion, that the reliability of saturated fluorescence as a technique for the measurement of molecular concentrations in atmospheric pressure flames has not yet been demonstrated.

Even for a low-pressure flame, where the influence of collision processes can be monitored, the interpretation of saturated fluorescence data is difficult. Non-uniform saturation over the collection volume occurs depending on the spatial laser beam profile. This has been described as Gaussian [10, 11] or truncated Gaussian [12]. These assumptions need not be true for the multi-mode lasers commonly used. Pulse-to-pulse variations of the spatial beam profile are likely to occur. Similarly, the temporal and spectral laser intensity profiles and their pulse-to-pulse fluctuations can influence the saturated fluorescence signal. Unless these effects can be considered correctly, accurate absolute number densities of radicals in flames cannot be obtained. In this work, we attempt to contribute to the improvement of the saturated fluorescence method.

Experiment

A schematic diagram of the experimental arrangement is shown in Fig. 1. A 13 mbar premixed acetylene/oxygen flame with an equivalence ratio of $\phi = 1.2$ was used for all experiments. The porous disk burner had a diameter of 20 mm and could be adjusted in height. Flow rates were measured with calibrated flow meters (Hastings EALK-1K) and stabilized by computer-controlling. The total flow rate was typically 650 cm^3 NTP/min.

A laser system (Quanta Ray) consisting of a Nd:YAG pump laser (DCR-1), a dye laser (PDL-1), and a frequency doubling and mixing unit (WEX 1) was used to excite the molecular species in the flame.

Ber. Bunsenges. Phys. Chem. *87*, 1052–1057 (1983) –
0005–9021/83/1111–1052 $ 02.50/0

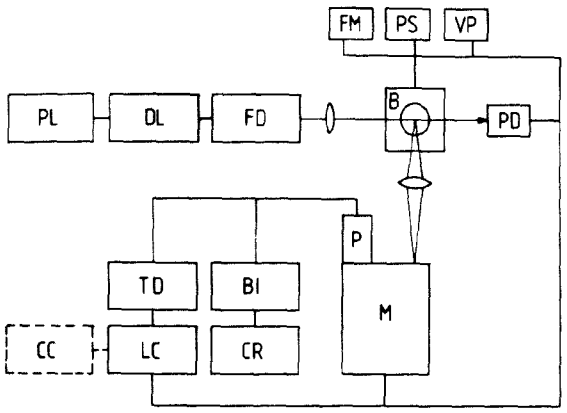

Fig. 1
Schematic diagram of the experimental arrangement.
B: burner in vacuum housing, FM: flow meters, PS: pressure sensor, VP: vacuum pump, PL: pump laser, DL: dye laser, FD: frequency doubler, PD: photodiode, M: monochromator, P: photomultiplier, BI: boxcar integrator, CR: chart recorder, TD: transient digitizer, LC: laboratory computer, CC: central computer

For CH excitation, a dye laser configuration with oscillator and side-pumped amplifier was used. They were both operated with a stilbene 3 (Lambda Physik) solution in methanol, which produced laser output around the $CH(A^2\Delta - X^2\Pi, 0\text{-}0)$ band head near 431 nm. For this pump geometry, a spatial beam profile of rather moderate quality was obtained. Therefore, only a small, more homogeneous portion of the beam was used.

OH excitation was performed with end-pumped amplifier geometry. A mixture of cresyl violet (Lambda Physik) and rhodamine 640 (Exciton) gave laser output around 630 nm, which was then doubled to match OH $(A^2\Sigma^+ - X^2\Pi, 0\text{-}0)$ band wavelengths near 315 nm. The laser beam was mildly focussed into the flame.

The laser intensity was monitored with a calibrated photodiode (ITT F 4000 S5). Typical laser pulses had halfwidths of about 5 ns. The laser energy per pulse, which was finally used for the excitation of CH, amounted to up to 0.25 mJ, whereas for OH excitation, up to 1 mJ in the UV-beam was reached. Pulse-to-pulse fluctuations in laser energy were measured to be less than 15% for the CH experiments; for the OH configuration, they were much higher due to the presently poor performance of our laser system.

Fluorescence was detected at right angles to the laser beam axis, but with an angle of 38 degrees with respect to the plane of the burner plate in order to decrease in the CH experiments the flame emission background. A mirror system and a lens focussed the fluorescence into the entrance slit of a 0.6 m monochromator (Jobin Yvon HRP). In our optical configuration, the length of the collection volume in the direction of the laser beam was given by the slit height, the collection volume diameter normal to it was determined by the slit width.

The fluorescence light was received by a photomultiplier (RCA 1 P28 or Hamamatsu R 928). Signals were recorded with a fast transient digitizer (Tektronix R 7912) with a minimal time resolution of ≤ 1 ns. For some experiments, a boxcar integrator with a minimal gate of 40 ns was used. The fluorescence data could be stored and processed in a PDP 11/05 laboratory computer or transferred to a PDP 11/44 computer for further evaluation.

Results and Discussion

For low-pressure flames with slow collisional deexcitation, a two-level system (Fig. 2) can be used as the simplest approach from which an expression for the radical number density can be deduced. At the beginning ($t = 0$), all molecules are in the lower state 1. The upper level is excited by absorption of the laser light, the population is decreased by stimulated emission, fluorescence, and collisional quenching. The time behaviour of the number density N_2 of the excited species can be given by

$$\frac{dN_2}{dt} = N_1 u_\nu B_{12} - N_2 \cdot (u_\nu B_{21} + A_{21} + Q_{21}) \quad (1)$$

where u_ν is the laser radiation density, B_{12}, B_{21} and A_{21} are the Einstein coefficients for absorption, stimulated, and spontaneous emission and Q_{21} is the quenching rate constant.

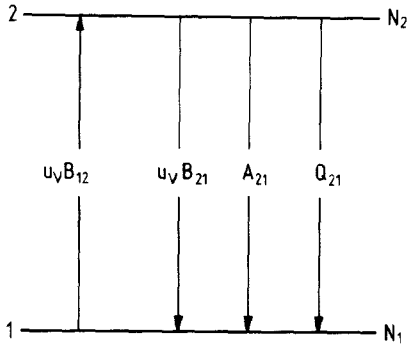

Fig. 2
Two-level system, see text

Though this rate equation expression is used very often, it is not necessarily valid for the applied high radiation densities with a mode structure of "monochromatic" lines within the overall bandwidth of the laser light [13]. Smith [14] gives a set of differential equations for the excitation of transitions between two atomic or molecular levels for monochromatic laser radiation and different line-broadening mechanisms. We solved his equations with the parameters given by our experiment. The multi-mode character of our laser was considered very approximately by adding an experimentally observed average laser linewidth to the natural linewidth of the transition, as suggested by Eberly [15]. With these assumptions, the difference between density matrix and rate equation calculations for our experimental conditions became negligible, so that Eq. (1) can be used with some justification. However, it should be noted that at present the theory of laser-induced excitation seems not quite satisfactorily developed with respect to the multi-mode excitation in many LIF experiments. Further theoretical work is urgently needed.

For a constant population

$$N_0 = N_1 + N_2 \quad (2)$$

and a rectangular laser pulse shape, integration of Eq. (1) gives

$$N_2 = \frac{N_0 \cdot (g_2/g_1) \cdot u}{[1 + (g_2/g_1)] \cdot u + \alpha} \cdot \{1 - \exp - (\langle [1 + (g_2/g_1)] \cdot u + \alpha \rangle \cdot \tau_L)\}; \quad t = \tau_L \quad (3)$$

with $u = u_\nu \cdot B_{21}$ and $\alpha = A_{21} + Q_{21}$. τ_L is the width of a rectangular laser pulse, which is assumed equal in height and area to the averaged experimental laser pulse. To justify this assumption, Eq. (1) was integrated for different intensities with a rectangular laser pulse of width τ_L as well as with a realistic, time-dependent laser pulse. For the latter, integration was performed until N_2/N_0 reached its maximum value at $t = t_{max}$ and then started to decay. Extrapolations of the exponential part of $N_2/N_0(t)$, valid for $t > t_{max}$, to the time τ_L gave the dashed line in Fig. 3. Compare also Fig. 4. As Fig. 3 shows, the

results did not differ markedly, so that Eq. (3) was used for further calculations.

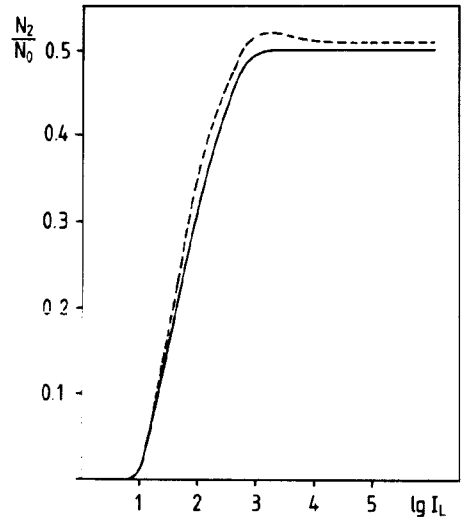

Fig. 3
Relative number density N_2/N_0 vs. laser intensity I_L (arbitrary units). —— solution of Eq. (1) with a rectangular laser pulse of width τ_L, integration limit τ_L. – – – solution of Eq. (1) with a realistic time-dependent laser pulse, see text. The maximum in the dashed curve is caused by the approximative nature of the extrapolation.

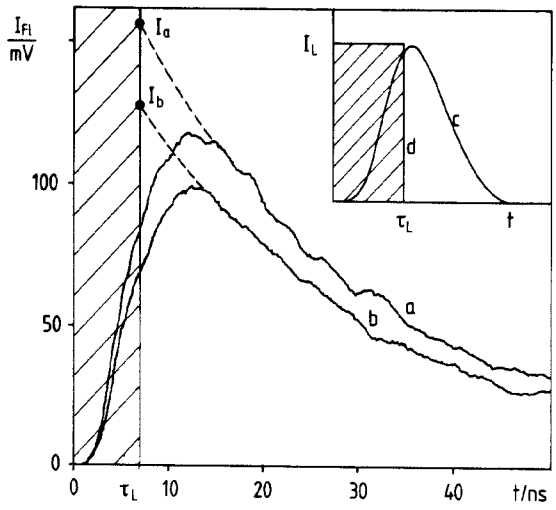

Fig. 4
Relative fluorescence intensity I_{FL} vs. time t. CH($A^2\Delta - X^2\Pi$, 0-0, R(6)) was monitored. The laser power was 10 KW for a 7 ns pulse, 200 pulses were averaged. a: without, b: with a filter of 50% transmission in the laser beam; I_a, I_b: see text.
Insert: Relative laser intensity I_L vs. time t. c: averaged experimental laser pulse, d: rectangular pulse of equal area and height as c. Width: τ_L

For complete saturation at $t = \tau_L$, Eq. (3) reduces to

$$N_{2,s} = \frac{N_0}{1 + (g_1/g_2)} \tag{4}$$

with $\alpha \ll u$, giving the highest possible population in level 2 independent of laser intensity and collision processes.

As the spatial laser intensity distribution is not homogeneous, different degrees of saturation in the collection volume have to be considered. With

$$V \equiv \int \frac{N_2(x,y,z)}{N_0}\,dx\,dy\,dz\,, \tag{5}$$

integration over the beam diameter gives

$$V = z \cdot \int \frac{(g_2/g_1)\cdot u \cdot f(x,y)}{[1 + (g_2/g_1)]\cdot u \cdot f(x,y) + \alpha} \cdot \{1 - \exp(\langle [1 + (g_2/g_1)]\cdot u \cdot f(x,y) + \alpha \rangle \cdot \tau_L)\} \cdot \frac{\Omega(x,y)}{\Omega_0}\,dx\,dy\,; \tag{6}$$

z is the observed length of the collection volume in the axis of the laser beam, $f(x,y)$ is a local intensity factor, and $\Omega(x,y)$ is a local imaging factor. The fluorescence intensity $I_{FL}^{\tau_L}$ and the number density N_0 are related by

$$I_{FL}^{\tau_L} = A_{21}\cdot h\cdot \nu \cdot \frac{\Omega_0}{4\pi}\cdot V \cdot N_0;\quad t = \tau_L\,, \tag{7}$$

ν being the fluorescence frequency and Ω_0 the collection angle. V is obtained from Eq. (6). The total species number density N_T can be evaluated from

$$N_T \simeq N_0/f_T;\quad f_T = \frac{g_1}{Q}\cdot \exp(-(E_1/kT)) \tag{8}$$

with the Boltzmann factor f_T, provided that the population in the lower level is thermal and the local temperature is known.

The experimental procedure was performed as follows. For several laser intensities the average saturation degree was measured. An example is shown in Fig. 4 which represents the time-dependent fluorescence intensity. Unlike the upper curve, the lower one was taken with a calibrated neutral density filter of 50% transmission in the laser beam. The ratio of the extrapolated fluorescence intensities I_b/I_a (Fig. 4) at the time τ_L gives an average saturation degree for the collection volume of 0.81 in this case.

Absolute fluorescence intensities were obtained by comparison with a calibration pulse of known intensity. The laser light was scattered by the surface of a grounded quartz disk. The wavelength and the imaging geometry were matched to those of the fluorescence. The scattered light was received either by a calibrated photodiode or by the photomultiplier used in the experiments.

The integral V (Eq. (6)) was calculated considering a two-dimensional field of average local intensity factors $f(x,y)$, which were measured by translating a pin-hole across the laser beam. In Fig. 5, the course of V with u is shown schematically; u is an expression for the laser intensity given by the following equations:

$$u = u_{\nu,\max}\cdot B_{21}\,, \tag{9}$$

$$I_L = c\cdot u_{\nu,\max}\cdot \int f(x,y)\,dx\,dy\cdot \int f(\nu)\,d\nu\,. \tag{10}$$

$f(x,y)$ is the spatial laser intensity distribution as above, $f(\nu)$ the spectral profile of the laser.

For low laser intensities, V increases linearly with u. For very high values of u, V approaches a saturation limit. The saturation degree S, which is obtained by a filter of 50% transmission in the laser beam, is given by

$$S = \frac{V(0.5\,u)}{V(u)}\,, \tag{11}$$

as indicated by the squares in Fig. 5. For linear conditions, S starts at 50%, for complete saturation S approaches 100%. For a given experimental value S_{exp}, the corresponding integral V_{exp} is obtained, and the number density N_0 can be calculated from Eq. (7).

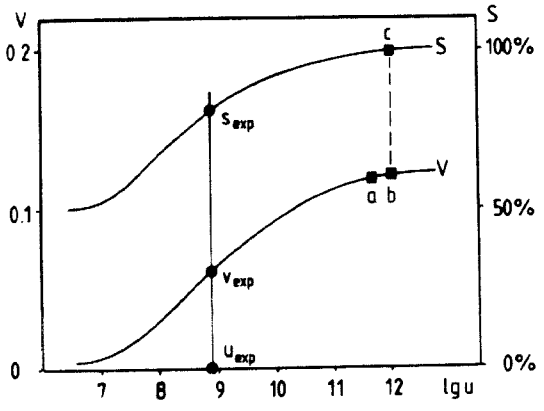

Fig. 5
Schematic diagram of integral V (Eq. (6)) and saturation degree S vs. laser intensity u.
Squares: example for the construction of the curve S from V (see Eq. (11)); a: $V(0.5\,u)$, b: $V(u)$, c: resulting S.
Circles: S_{exp}: measured saturation degree (example of Fig. 4); V_{exp}: corresponding integral V from which the number density is calculated; u_{exp}: corresponding laser intensity u from which the approximate oscillator strength is determined.

From the intercept u_{exp}, an approximate oscillator strength f_{12} can be determined. f_{12} is defined as follows:

$$f_{12} = \frac{4 m_e \cdot h \cdot \varepsilon_0 \cdot \nu}{e^2} \cdot \frac{g_1}{g_2} \cdot B_{21}\,; \qquad (12)$$

B_{21} is obtained from Eq. (9) with $u = u_{exp}$, $u_{\nu,max}$ is expressed by experimental parameters (Eq. (10)). Oscillator strengths for the CH [16] and OH [17] bands considered in the experiments are well-known. As an advantage of our method, we thus have the possibility to check the validity of the assumptions used for the determination of the number densities.

Fig. 6 represents the results of a CH experiment with excitation of Q(7) and observation of R(6). About 70 measured degrees of saturation are displayed for 3 1/2 orders of magnitude in u. For this case, a four-level model had to be used, as within the laser bandwidth, $Q^{0,0}(7)$ and $Q^{1,1}(7)$ were excited. Because of the laser being centered on the (0,0) transition and detuned from the (1,1) Q(7) line, the latter was saturated at higher laser intensities as the (0,0) Q(7) line, causing the bend in V and the plateau in S (Fig. 6).

Table I shows the calculated number densities for this experiment in the first column. For the four-level system indicated in the first line, 200 ppm of CH were measured with a statistical deviation of ±25%. This number density corresponds to a height h of 2.3 mm above the surface of the burner, where the CH maximum was found, and a measured temperature of 1750 K. As shown in the second column of Table I, an equivalent experiment for a two-level system resulted in a very good agreement for the CH concentration. The approximate oscillator strengths determined from both experiments were equal to the

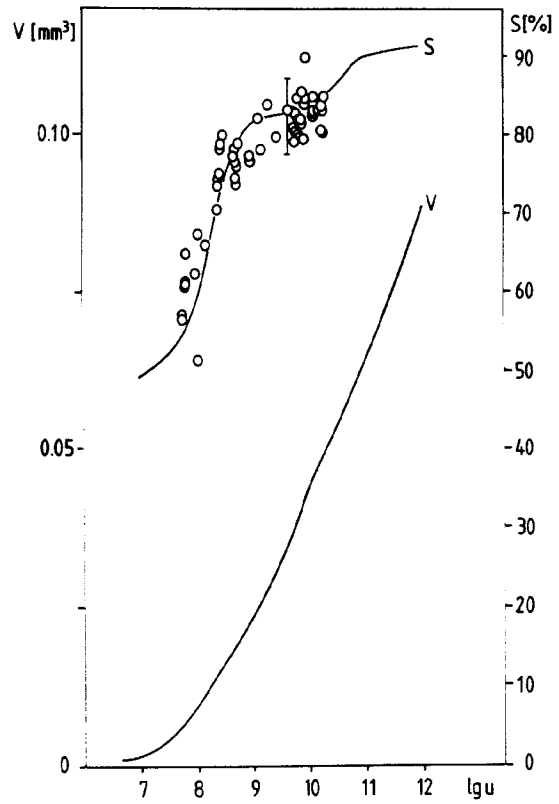

Fig. 6
Integral V and saturation degree S vs. laser intensity u. CH($A^2\Delta - X^2\Pi$) $Q^{0,0}(7)$ and $Q^{1,1}(7)$ were excited, $R^{0,0}(6)$ and $R^{1,1}(6)$ were monitored at h = 2.3 mm above the burner surface in a 13 mbar, ϕ = 1.2 $C_2H_2 - O_2$ flame with a local temperature of 1750 K in the collection volume.

value of Becker et al. [16] within an factor of two, corresponding to the accuracy which may be expected for the extrapolation in our experiment.

Table I
CH and OH number densities determined by saturated fluorescence for a 13 mbar, ϕ = 1.2 $C_2H_2 - O_2$ flame

Molecule	CH	CH	OH
spectral line system	$A^2\Delta - X^2\Pi$	$A^2\Delta - X^2\Pi$	$A^2\Sigma^+ - X^2\Pi$
excitation	$Q^{0,0}(7)$, $Q^{1,1}(7)$	$P^{0,0}(7)$	$Q_2^{0,0}(17)$
observation	$R^{0,0}(6)$, $R^{1,1}(6)$	$R^{0,0}(5)$	$P_2^{0,0}(18)$
height above burner surface	2.3 mm	2.3 mm	7.5 mm
temperature	1750 K	1750 K	2000 K
number density	$1.1 \cdot 10^{13}$/cm³ (±25%)	$1.1 \cdot 10^{13}$/cm³ (±20%)	$8.9 \cdot 10^{14}$/cm³ (±30%)
mole fraction	200 ppm	200 ppm	18500 ppm
oscillator strength			
experiment	$(2.5-10) \cdot 10^{-3}$	$(2.5-10) \cdot 10^{-3}$	$(0.1-1.1) \cdot 10^{-3}$
references	$5.2 \cdot 10^{-3}$ [16]	$5.2 \cdot 10^{-3}$ [16]	$1.1 \cdot 10^{-3}$ [17]

The last column of Table I shows the results for OH. Due to the presently large pulse-to-pulse intensity fluctuations of our laser, the experimental error is higher than for CH, and a

systematical deviation of the oscillator strength of a factor of 3.5 from Ref. [17] is found. Therefore, we additionally used the linear fluorescence method described by Stepowski and Cottereau [18] and the Baronavski-McDonald [3] extrapolation for near saturation. As displayed in Table II, the results of all three methods agreed very well.

Table II
OH number densities obtained from different methods

saturated fluorescence, this work	$8.9 \cdot 10^{14}/cm^3$
saturated fluorescence, Baronavski-McDonald [3] extrapolation	$1.0 \cdot 10^{15}/cm^3$
linear fluorescence method of Stepowski and Cottereau [18]	$8.3 \cdot 10^{14}/cm^3$

The local temperature needed for these evaluations at the maximum concentrations of CH and OH was measured separately as explained in the next section.

Comparison with a Flame Model

The experimental number densities for OH and CH were compared with those obtained from a kinetic $C_2H_2-O_2$ model [19]. The results are displayed in Fig. 7. The upper curve (a) shows the temperature profile of our flame which was used for the simulation. Laser-induced fluorescence temperature measurements are not without problems. Non-thermal populations can cause large systematic errors [17a, 20], and therefore relaxation models may be required [21, 22], or a very high precision is necessary for two-line molecular temperature measurements [23, 24]. In this work, CH and OH rotational temperatures of the excited molecule were determined after a sufficient time delay with respect to the laser pulse, so that the population had thermalized; the comparison with radiation corrected [25] thermocouple measurements shows good agreement.

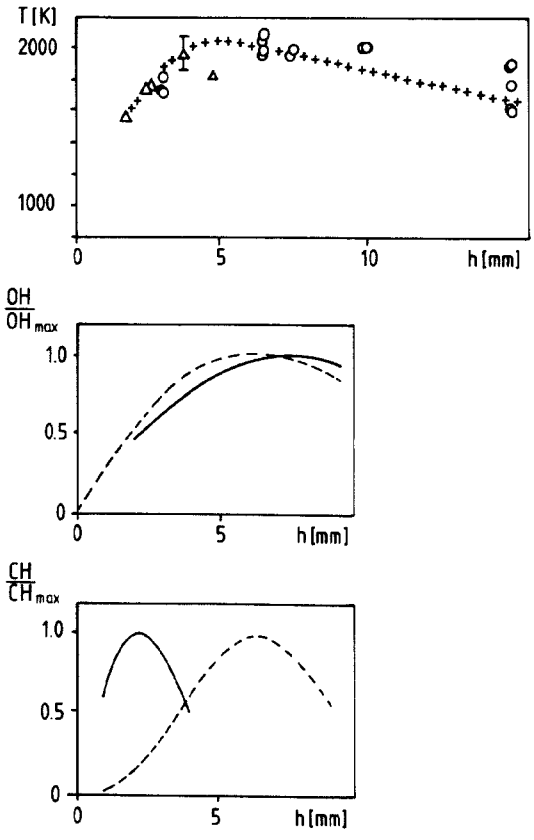

Fig. 7
a) Temperature T vs. height h above the burner surface;
○: OH rotational temperatures,
△: CH rotational temperatures,
+: radiation corrected [25] thermocouple measurements;
b) normalized measured (—) and simulated (– – –) OH profiles; the latter has to be multiplied by a factor of 0.9.
c) normalized measured (—) and simulated (– – –) CH profiles; the latter has to be multiplied by a factor of 1.4.

The second curve (7b) shows that measured and simulated OH profile agree quite well. It is known that OH simulation even in an acetylene flame can now successfully be done [26], so that it can serve as control. Furthermore, very similar OH number densities have been found in hydrogen [7b] and propane [18] low-pressure flames. Our CH results do not agree very well with the present model predictions (Fig. 7c). This reflects simply our present lack of knowledge of qualitative and quantitative data for CH production and consumption in an $C_2H_2-O_2$ flame. Our experimental results will be used in an attempt to improve the CH-submodel in the $C_2H_2-O_2$ kinetic scheme. The reactions governing the formation and consumption of CH in the present model are shown in Table III.

Table III
Kinetic submodel for the production and consumption of CH in the $C_2H_2-O_2$ flame following Warnatz [19]. $K = A \cdot T^b \cdot \exp -(E/kT)$

Elementary reaction	A ($cm^3\ mol^{-1}\ s^{-1}$)	b	E($kJ\ mol^{-1}$)
$C_2H_2 + O \rightarrow CH_2 + CO$	$4.1 \cdot 10^8$	1.5	7.1
$CH_2 + H \rightarrow CH + H_2$	$4 \cdot 10^{13}$	–	–
$CH + O \rightarrow CO + H$	$5.7 \cdot 10^{13}$ [a]	–	–
$CH + O_2 \rightarrow CO + OH$	$3.6 \cdot 10^{13}$ [b]	–	–
$CH + C_2H_2 \rightarrow C_3H_3$	$2.4 \cdot 10^{14}$ [c]	–	–

[a] I. Messing, T. Carrington, S. V. Filseth, and C. M. Sadowski, Chem. Phys. Lett. *74*, 56 (1980).
[b] J. E. Butler, J. W. Fleming, L. P. Goss, and M. C. Lin, in: Laser Probes for Combustion Chemistry (ed. D. R. Crosley), Am. Chem. Soc. Symp. Series, p. 397, Vol. 134 (1980).
[c] M. R. Berman, J. W. Fleming, A. B. Harvey, and M. C. Lin, Chem. Phys. *73*, 27 (1982).

Flames at Higher Pressures

As mentioned before, for the extension of our method to higher pressures, relaxation processes have to be considered. There are only few state-to-state relaxation constants available for the important flame radicals [27], and as measurements for different flame conditions would be very time-consuming, several attempts have been made [22, 28–30] to model the relaxation processes. Some preliminary results of our multilevel model, whose parameters are shown in Table IV, are displayed in Fig. 8. Quite good agreement of the observed CH spectra and of their time development with the model was obtained by using the following assumptions, which seem reasonable from various experiments:

(a) rotational energy transfer of more than one quantum was considered,
(b) transfer probabilities were modelled using a combined exponential and power law, so that the probability

decreases with increasing quantum number and with increasing amount of quanta transferred,

(c) rotational relaxation was assumed to be faster than quenching, vibrational relaxation was neglected for the example in Fig. 8 as being too slow on the time-scale considered.

It will be necessary to investigate further, whether this simple model will hold also for different radicals and flame conditions.

Table IV
Relaxation model

Number of rotational levels	15 in upper, 15 in lower electronic state, non-degenerate
initial concentrations	thermal; upper state: relative population due to flame chemistry estimated from CH emission signal (without laser)
spontaneous emission	P, Q, R branches considered with probabilities given by Hönl-London factors
quenching	equal probabilities for all upper levels
absorption, stimulated emission	time-dependent laser pulse $u = a \cdot t^b \cdot e^{-ct}$, spatial intensity distribution approximated by six intensity steps
rotational relaxation	combined exponential/power law downward transfer: $R_{ji} = R_0 \cdot \exp[-(\Delta E/\alpha_R)^d]$ upward transfer: detailed balancing transfer of up to five quanta R_0, α_R, d equal for upper and lower states

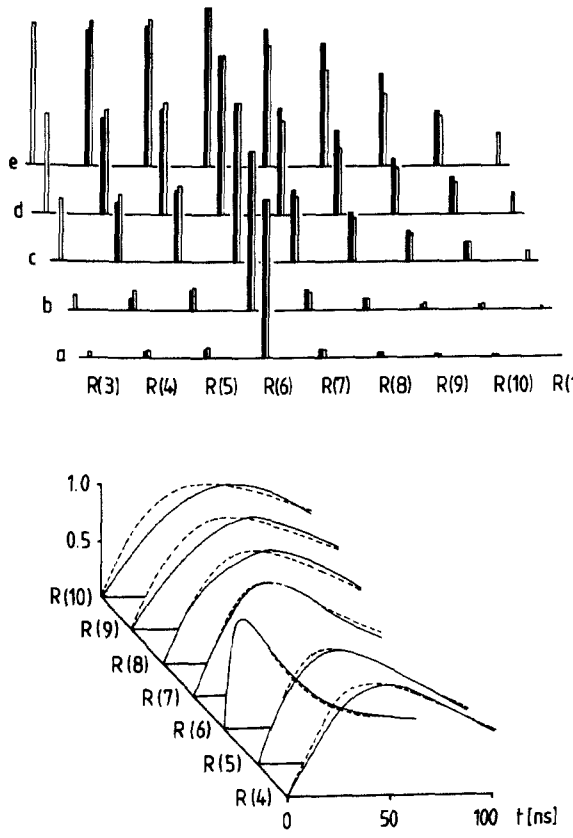

Fig. 8
Schematically displayed CH spectra (top) and their time development (bottom) in a 13 mbar $C_2H_2-O_2$-flame.
—, ■ experiment; – – –, □ relaxation model;
a: t = 10 ns, b: 20 ns, c: 50 ns, d: 70 ns, e: 100 ns

Conclusions

An attempt was made to demonstrate that the method of laser-induced saturated fluorescence can be applied for the determination of radical concentrations in low-pressure flames, provided that the validity of some assumptions which have been discussed in the text can be verified. The extension of the method to higher pressures implies the knowledge of state-to-state relaxation constants or the description of such collision processes by adequate modelling.

We express our thanks to Dr. M. Mailänder who started with the development of the method for discussions. We thank Mr. P. Koczar who performed the OH-experiments for his skillful assistance.

References

[1] E. H. Piepmeier, Spectrochim. Acta *27B*, 431 (1972).
[2] J. W. Daily, Appl. Opt. *16*, 568 (1977).
[3] A. P. Baronavski and J. R. McDonald, J. Chem. Phys. *66*, 3300 (1977); Appl. Opt. *16*, 1897 (1977).
[4] M. Mailänder, J. Appl. Phys. *49*, 1256 (1978).
[5] P. A. Bonczyk and J. A. Shirley, Combust. Flame *34*, 253 (1979).
[6] J. F. Verdieck and P. A. Bonczyk, 18th Symp. (Int.) on Combustion, p. 1559, The Combustion Institute, Pittsburgh, Penn. 1981.
[7] a) R. P. Lucht, D. W. Sweeney, and N. M. Laurendeau, in: Laser Probes for Combustion Chemistry (ed. D. R. Crosley) Am. Chem. Soc. Symp. Series, Vol. 134, p. 145 (1980); b) to appear in Combust. Flame (1983).
[8] J. T. Salmon, R. P. Lucht, N. M. Laurendeau, and D. W. Sweeney, 1982 October Meeting, Western States Section, The Combustion Institute, Livermore, California, USA.
[9] C. Morley, Combust. Flame *47*, 67 (1982).
[10] J. W. Daily, Appl. Opt. *17*, 225 (1978).
[11] M. B. Blackburn, J.-M. Mermet, G. D. Boutilier, and J. D. Winefordner, Appl. Opt. *18*, 1804 (1979).
[12] L. Pasternack, A. P. Baronavski, and J. R. McDonald, J. Chem. Phys. *69*, 4830 (1978).
[13] J. W. Daily, Appl. Opt. *16*, 2322 (1977).
[14] R. A. Smith, Proc. R. Soc. London *A 362*, 1 (1978); Proc. R. Soc. London *A 362*, 13 (1978); Proc. R. Soc. London *A 368*, 163 (1979); Proc. R. Soc. London *A 371*, 319 (1980).
[15] J. H. Eberly, in: Laser Spectroscopy IV, p. 80 (ed. H. Walther and K. W. Rothe), Springer, Berlin, Heidelberg, New York 1979.
[16] K. H. Becker, H. H. Brenig, and T. Tatarczyk, Chem. Phys. Lett. *71*, 242 (1980).
[17] a) G. P. Smith and D. R. Crosley, 18th Symp. (Int.) on Combustion, p. 1511, The Combustion Institute, Pittsburgh, Penn. 1981, recommend the results of b) K. R. German, J. Chem. Phys. *62*, 2584 (1975) and c) W. L. Dimpfl and J. L. Kinsey, J. Quant. Spectrosc. Radiat. Transfer *21*, 233 (1979).
[18] D. Stepowski and M. J. Cottereau, Appl. Opt. *18*, 354 (1979).
[19] J. Warnatz, personal communication.
[20] D. R. Crosley, Opt. Eng. *20*, 511 (1981).
[21] C. Chan and J. W. Daily, Appl. Opt. *19*, 1963 (1980).
[22] D. R. Crosley and G. P. Smith, Combust. Flame *44*, 27 (1982).
[23] R. J. Cattolica, Appl. Opt. *20*, 1156 (1981).
[24] R. P. Lucht, N. M. Laurendeau, and D. W. Sweeney, Appl. Opt. *21*, 3729 (1982).
[25] W. E. Kaskan, 6th Symp. (Int.) on Combustion, p. 134, Reinhold Publishing Corp., New York 1957.
[26] J. Warnatz, 18th Symp. (Int.) on Combustion, p. 369, The Combustion Institute, Pittsburgh, Penn. 1981.
[27] R. K. Lengel and D. R. Crosley, J. Chem. Phys. *67*, 2085 (1977).
[28] J. O. Berg and W. L. Shackleford, Appl. Opt. *18*, 2093 (1979).
[29] R. P. Lucht, D. W. Sweeney, and N. M. Laurendeau, Appl. Opt. *19*, 3295 (1980).
[30] C. Chan and J. W. Daily, Appl. Opt. *19*, 1357 (1980).

E 5512